Bulgarian Chemical Communications, Volume 58, Issue 2 (pp. 200-208) 2026 DOI: 10.34049/bcc.58.2.NCC04

Computational evaluation of COX-1 binding by EPA, DHA, and AA using blind and flexible docking approaches

R. Stancheva[1*], I. Iliev[2], A. Merdzhanova[1], S. Georgieva[2]

[1]*Department of Chemistry, Faculty of Pharmacy, Medical University of Varna, Bulgaria*
[2]*Department of Pharmaceutical Chemistry, Faculty of Pharmacy, Medical University of Varna, Bulgaria*

Received: October 22, 2025; Revised: March 16, 2026

Omega-3 polyunsaturated fatty acids (PUFAs), including eicosapentaenoic acid (EPA) and docosahexaenoic acid (DHA), are associated with anti-inflammatory effects, but their molecular interactions with cyclooxygenase-1 (COX-1) remain incompletely understood. This study employed blind and flexible molecular docking simulations using AutoDock 4.2 to assess the binding of EPA, DHA, and arachidonic acid (AA) to COX-1 (PDB ID: 6Y3C). In rigid blind docking, DHA exhibited the strongest predicted affinity (−7.83 kcal/mol, Ki = 1.82 μM), followed by EPA (−7.21 kcal/mol, Ki = 5.21 μM) and AA (−6.11 kcal/mol, Ki = 33.11 μM), although none of the ligands engaged the catalytic residues, and high RMSD values indicated broad conformational sampling. Flexible docking, allowing selected active site residues (ARG120, TYR355, LEU384, TYR385, ILE523) to move, repositioned all ligands within the catalytic pocket, yielding improved binding energies (ΔG = −9.09 kcal/mol for AA, −9.03 kcal/mol for EPA, and −8.73 kcal/mol for DHA) and nanomolar inhibition constants. EPA closely reproduced the AA binding pose (RMSD = 3.90 Å), while DHA adopted a distinct but favorable orientation (RMSD = 5.37 Å). Both ω-3 PUFAs formed hydrogen and hydrophobic interactions with key residues (ARG120, TYR355, TYR385, SER530), consistent with competitive engagement of the catalytic site. These results indicate that EPA and DHA can stably interact with COX-1, supporting a mechanistic basis for their anti-inflammatory properties, and underscore the importance of receptor flexibility in accurately modeling enzyme-ligand interactions. Further studies, including molecular dynamics simulations and experimental validation, are warranted to confirm these findings and elucidate the mechanistic basis of ω-3 fatty acids' anti-inflammatory effects.

Keywords: Omega-3 fatty acids, Cyclooxygenase-1 (COX-1), Blind rigid-body docking, AutoDock 4.2, Anti-inflammatory potential, Flexible docking

INTRODUCTION

Cyclooxygenase-1 (COX-1) is a constitutively expressed enzyme that plays an important role in the biosynthesis of prostaglandins from arachidonic acid (AA), thereby contributing to a variety of physiological processes such as gastric protection, platelet aggregation, and renal function [1-3]. COX-1 is one of three isoforms – alongside COX-2 and COX-3 – each of which exhibits distinct expression patterns and biological roles [1, 2].

Structurally, COX-1 exists as a homodimer, and each monomer contains a large globular catalytic domain with an active site shaped as an inverted L-channel composed mainly of hydrophobic residues [3-5]. This active site can be subdivided into proximal, central, and distal pockets which cooperate to stabilize and position AA during catalysis [4, 5]. One of the key residues governing ligand selectivity in COX-1 is isoleucine at position 523, distinguishing it from COX-2, where valine at this site confers greater flexibility and substrate access [1, 6]. This structural divergence has been exploited in the development of selective COX-2 inhibitors and underscores the pharmacological significance of understanding COX-1-ligand interactions [1, 2].

In recent years, the anti-inflammatory potential of omega-3 polyunsaturated fatty acids (PUFAs) – particularly eicosapentaenoic acid (EPA) and docosahexaenoic acid (DHA) – has attracted considerable scientific attention. These long-chain fatty acids are essential components of cell membranes and serve as precursors for a variety of bioactive lipid mediators that modulate inflammatory responses, neuroprotection, and immune regulation [7-10]. Unlike AA which gives rise to pro-inflammatory eicosanoids, EPA and DHA are generally associated with the production of less inflammatory or even anti-inflammatory derivatives [8, 9]. For example, DHA has been implicated in promoting neurite growth and maintaining cognitive function, while EPA-derived lipid mediators exhibit reduced potency in eliciting inflammation compared to their AA-derived counterparts [7, 9].

The metabolic pathways of these fatty acids are tightly interconnected. AA is synthesized from linoleic acid, while EPA and DHA are derived from α-linolenic acid through desaturation and elongation,

* To whom all correspondence should be sent:
Email: *rositsa.stancheva@mu-varna.bg*

although conversion rates in humans are low, making dietary intake crucial [9, 10]. Retroconversion of DHA can also produce EPA and docosapentaenoic acid (DPA), adding another layer of metabolic interplay [10]. Of particular interest are electrophilic fatty acid oxo-derivatives, a novel class of endogenous anti-inflammatory molecules derived from EPA, DHA, and DPA, which can activate PPARγ and inhibit pro-inflammatory cytokines [7]. These findings highlight the relevance of omega-3 fatty acids as modulators of inflammation.

Despite the growing body of literature supporting the anti-inflammatory potential of omega-3 fatty acids, questions remain regarding their direct competitive behavior with AA at the active site of COX-1 [11]. While many studies have investigated downstream metabolic effects and systemic outcomes, comparatively fewer have addressed the molecular details of how long-chain polyunsaturated fatty acids interact with COX-1 at the binding-site level. Previous experimental work has largely focused on prostaglandin production and substrate availability, without evidence for altered COX-1 or COX-2 expression [12]. In parallel, recent biochemical and structural studies have demonstrated that cyclooxygenase enzymes possess both catalytic and allosteric sites capable of accommodating fatty acids and small-molecule ligands [13].

To address this gap, computational approaches such as molecular docking offer valuable tools for elucidating ligand-enzyme interactions at the atomic level. Docking techniques predict the binding affinity and pose of a ligand within the active site of a target protein, and are widely used in early-stage drug discovery and mechanistic studies [14]. Among the various strategies, rigid-body docking is computationally efficient and assumes that both the ligand and the receptor remain static during interaction [15-17]. A subtype of this method, blind docking, involves scanning of the entire protein surface without predefined binding-site information, allowing for unbiased identification of potential ligand-accessible pockets [18-20]. Although blind docking is more computationally intensive, it is particularly useful when the ligand's binding site is unknown or when allosteric interactions are being considered [14, 18].

However, flexible docking approaches provide a more realistic representation of biological binding by allowing conformational adjustments in selected amino acid residues or even in the entire active site during ligand accommodation [21]. This dynamic treatment of the receptor enables better modeling of induced-fit effects and can reveal binding modes inaccessible to rigid-body docking. Consequently, flexible docking is often employed as a refinement step following initial rigid or blind docking analyses, improving the accuracy of predicted binding poses and interaction energies [22].

This study employs blind rigid-body and flexible docking to computationally evaluate and compare the binding of AA, EPA, and DHA to the active site of COX-1. By applying AutoDock-based protocols, the aim is to assess whether omega-3 fatty acids can effectively compete with AA for enzymatic binding and to what extent their binding affinities and predicted interaction profiles provide molecular-level insight into potential competitive interactions with arachidonic acid at COX-1. The results may offer mechanistic insights into how EPA and DHA interact with COX-1 at the molecular level and contribute to a deeper understanding of their anti-inflammatory potential through interference with arachidonic acid metabolism.

MATERIALS AND METHODS

Three ligands – eicosapentaenoic acid (EPA), docosahexaenoic acid (DHA), and arachidonic acid (AA) – were selected for molecular docking based on their established involvement in inflammatory signaling pathways. The 3D structures of all compounds were retrieved from the PubChem database [23] in SDF format. Each ligand is imported into Avogadro [24], where geometry optimization is performed using the “Optimize Geometry” function to obtain low-energy conformations. The optimized structures were then saved in MOL2 format and subsequently loaded into AutoDock Tools [21]. Polar hydrogens were added, Gasteiger charges were assigned, rotatable bonds were detected, and the ligands were saved in PDBQT format for docking.

The crystal structure of cyclooxygenase-1 (COX-1) was obtained from the RCSB Protein Data Bank (PDB ID: 6Y3C) [25, 26]. 6Y3C represents the only available experimentally resolved structure of human COX-1. Other human cyclooxygenase structures deposited in the PDB correspond to the COX-2 isoform, while the majority of COX-1 structures originate from ovine sources. Accordingly, 6Y3C was selected to ensure human isoform specificity and to avoid species-dependent structural variations in the cyclooxygenase channel. Initial preprocessing was conducted using UCSF ChimeraX [27], where all non-standard residues were removed. The protein was then imported into AutoDock Tools, where water molecules were deleted, missing atoms were verified and corrected and polar hydrogen atoms were added. Kollman

charges were assigned, atom types were set according to the AD4 specification, and the protein was saved in PDBQT format.

Molecular docking simulations were carried out using AutoDock 4.2 with the Lamarckian Genetic Algorithm. Two complementary docking strategies were applied for each ligand – blind rigid-body docking and flexible docking – to ensure both global and localized exploration of potential binding modes. In the blind docking protocol, a large grid box encompassing the entire enzyme surface was defined to allow unrestricted ligand exploration. Each ligand-protein pair was subjected to 100 independent docking runs, with a population size of 150, a mutation rate of 0.02, a crossover rate of 0.8, and a maximum of 25,000,000 energy evaluations per run. The best binding pose for each ligand was selected based on the lowest predicted binding free energy (ΔG). Since the docking was performed with a rigid protein structure and a blind search across the entire macromolecular surface, the generation of dispersed conformational clusters and higher RMSD values was anticipated. For this reason, RMSD-based convergence was not used as a strict selection criterion for pose selection in blind docking.

The purpose of blind docking in this study was to assess the global binding preferences of AA, EPA, and DHA across the entire COX-1 surface in an unbiased manner. This approach allows evaluation of whether the canonical cyclooxygenase channel is energetically favored relative to other hydrophobic regions of the enzyme prior to focused docking simulations. For the flexible docking simulations, a focused grid centered at coordinates x = –31.521, y = –45.301, z = 5.179, with grid spacing 0.375 Å, was applied to target the enzyme's catalytic site. The same algorithmic parameters and number of docking runs (100) were maintained to ensure comparability. The following residues were defined as flexible to account for induced-fit effects: ARG120, TYR355, LEU384, TYR385, ILE523, and SER530. The population size for the flexible docking runs was increased to 300 to enhance conformational sampling within the active site.

To validate the docking protocol, the co-crystallized molecule present in the human COX-1 crystal structure (PDB ID: 6Y3C), FLC (citrate ion), was extracted and re-docked into a focused grid centered on its crystallographic position within the protein. It should be noted that the co-crystallized molecule labeled FLC in the 6Y3C structure corresponds to citrate ion, present as three copies originating from the crystallization buffer. These ions do not occupy the enzyme's canonical cyclooxygenase channel and are not considered biologically relevant ligands for COX-1. Nevertheless, 6Y3C was retained as the receptor model, as it represents the only experimentally resolved crystal structure of human COX-1 in the Protein Data Bank. The use of FLC in the re-docking validation was limited to geometric pose reproduction, assessing the protocol's ability to recover the crystallographic placement of the molecule within the protein matrix, irrespective of its biological role.

Re-docking was carried out using AutoDock 4.2 with a focused grid centered on the crystallographic position of the citrate ion (grid spacing 0.375 Å), employing the same Lamarckian Genetic Algorithm parameters as used in the flexible docking simulations, with validation based on geometric pose reproduction. The top-ranked docked pose was compared to the experimental crystallographic pose by calculating the heavy-atom RMSD. The validation was based on pose reproduction rather than a detailed interaction analysis, as the primary objective was to assess the geometric reliability of the docking protocol. The resulting RMSD of 1.739 Å confirms the geometric reliability of the AutoDock 4.2 setup and parameterization, demonstrating the consistency of the docking algorithm in recovering crystallographic poses and supporting its application for the subsequent focused docking of AA, EPA, and DHA within the catalytic site. Protocol validation was thus based solely on geometric pose reproduction of FLC, independently of its biological relevance. For all subsequent comparative analyses, arachidonic acid (AA) – the endogenous substrate of COX-1 – served as the primary biological reference ligand.

Inhibition constants (Ki) were estimated by AutoDock 4.2 from predicted binding free energies using its built-in thermodynamic conversion ($\Delta G = RT \ln Ki$, where $R = 1.987 \times 10^{-3}$ kcal/mol·K and T = 298 K). The resulting Ki values are theoretical estimates used for relative comparison. AA was used as a reference ligand for comparative analysis to evaluate the biological relevance and spatial accuracy of docking results. Comparative analyses included spatial overlap and relative orientation of docked EPA and DHA poses with respect to the docked AA reference within the COX-1 catalytic channel.

For comparative analysis of ligand positioning within the COX-1 catalytic pocket, the reference configuration was defined as the top-ranked docked pose of arachidonic acid (AA) obtained from the flexible docking protocol. All ligand-protein complexes were first aligned based on the COX-1

backbone to ensure a common structural reference frame.

Post-docking analyses were performed using UCSF ChimeraX and Discovery Studio Visualizer [28] to examine ligand-protein interactions, including hydrogen bonding, hydrophobic contacts, and steric complementarity. The spatial orientation of each ligand was analyzed with respect to catalytically relevant residues of COX-1, particularly LEU117, ARG120, PHE205, VAL344, TYR385, and SER530. Interaction profiles were used to assess whether omega-3 fatty acids form stable complexes in proximity to, or overlapping with, the enzyme's functional site.

RESULTS AND DISCUSSION

Both blind and flexible docking simulations were performed to assess the binding characteristics of DHA, EPA, and AA toward COX-1. Blind docking was used to identify potential surface-accessible binding sites, while flexible docking was employed to refine ligand placement within the catalytic pocket by allowing conformational mobility of selected residues.

Blind rigid-body docking results

Molecular docking simulations revealed that both omega-3 fatty acids exhibit stronger binding affinities to COX-1 compared to AA. DHA showed the most favorable binding profile, with a predicted binding energy (ΔG) of −7.83 kcal/mol and an estimated inhibition constant (Ki) of 1.82 μM. EPA followed with a ΔG of −7.21 kcal/mol and Ki of 5.21 μM. In contrast, AA showed the weakest interaction, with a ΔG of −6.11 kcal/mol and a significantly higher Ki of 33.11 μM. Intermolecular energy values further supported this trend, with DHA exhibiting the most stabilizing interactions (−12.30 kcal/mol), followed by EPA (−11.38 kcal/mol) and AA (−10.59 kcal/mol). These results suggest that DHA and EPA may form more stable complexes with COX-1 than the endogenous substrate AA, which is consistent with their proposed anti-inflammatory potential. A complete summary of the docking results, including electrostatic, internal, and torsional energy components, is presented in Table 1.

The predicted binding free energy (ΔG) serves as a thermodynamic estimate of how strongly a ligand interacts with its target under simulated conditions. More negative ΔG values typically indicate the formation of energetically favorable and stable ligand-receptor complexes, which may correlate with the higher inhibitory potential in biochemical systems [22]. In this context, the relatively low ΔG values observed for the omega-3 fatty acids suggest that they are capable of establishing stable interactions with COX-1, possibly outcompeting the natural substrate arachidonic acid. The estimated inhibition constants reinforce this interpretation, as lower Ki values are indicative of stronger binding affinity and greater likelihood of effective enzyme modulation. When Ki falls within the low micromolar range – as is this case – it is generally considered biologically relevant and compatible with physiological ligand concentrations [29, 30]. These findings support the hypothesis that omega-3 fatty acids may act as competitive modulators of COX-1-mediated inflammatory signaling.

To gain further insight into the nature of these interactions, the ligand-protein binding profiles were examined in detail. DHA forms three hydrogen bonds – with CYS41, GLN44, and HIS43 – alongside extensive hydrophobic contacts involving CYS36, CYS47, PRO40, PRO153, PRO156, LEU152, and ARG469. EPA, while forming only a single hydrogen bond with CYS47, engages in multiple alkyl interactions with residues such as CYS36, CYS41, PRO153, and PRO156. Arachidonic acid similarly forms a hydrogen bond with CYS41 and hydrophobic interactions with CYS47, PRO153, ILE46, LEU152, and PRO125.

Despite some overlap in the interacting residues – particularly CYS41, CYS47, and PRO153 – all three ligands bind outside the canonical catalytic pocket of COX-1, which includes ARG120, TYR385, SER530, and neighboring residues critical for substrate binding and enzymatic activity [31]. This observation is consistent with the rigid-body docking approach employed, which does not account for protein flexibility or induced fit effects that may be required for productive orientation within the active site.

Blind docking revealed multiple energetically favorable binding regions outside the canonical catalytic channel, motivating subsequent focused flexible docking to directly probe ligand behavior within the enzymatic pocket.

Nevertheless, the broader and more diverse interaction network formed by DHA, including multiple hydrogen bonds and stabilizing hydrophobic contacts, suggests a more extensive and potentially favorable surface interaction pattern compared to EPA and AA. EPA shows a similar, albeit less extensive, interaction pattern, while AA displays the least complex interaction profile. These differences further support the view that omega-3 fatty acids may occupy functionally relevant surface regions of COX-1 and interact with COX-1 through non-classical surface binding modes. The ligand-protein interaction profiles for DHA, EPA, and AA are shown in Figure 1.

Table 1. Summary of blind docking results for DHA, EPA, and AA with COX-1.

Ligand	Binding energy ΔG, kcal/mol	Ki, μM	Intermolecular energy, kcal/mol	Electrostatic energy, kcal/mol	Torsional free energy, kcal/mol	Internal energy, kcal/mol
DHA	−7.83	1.82	−12.30	−0.20	4.47	−1.35
EPA	−7.21	5.21	−11.38	−0.16	4.18	−1.18
AA	−6.11	33.11	−10.59	−0.19	4.47	−0.96

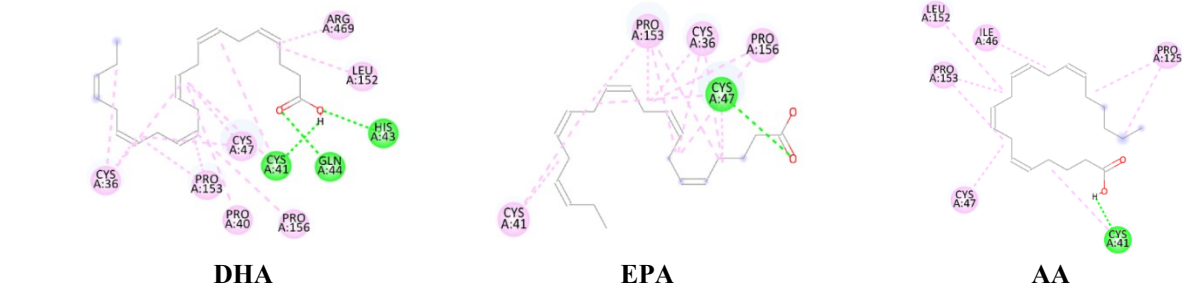

Figure 1. Two-dimensional interaction diagrams from blind docking of docosahexaenoic acid (DHA), eicosapentaenoic acid (EPA), and arachidonic acid (AA) bound to COX-1, illustrating conventional hydrogen bonds (green) and alkyl interactions (pink).

Although none of the three ligands directly engages catalytically essential residues, their consistent interaction with overlapping peripheral residues suggests a common binding surface on COX-1. The absence of active-site contacts is likely a consequence of the rigid-body docking approach, which does not account for protein flexibility or induced fit. However, given the stronger binding energies of DHA and EPA compared to AA, along with their spatial overlap in surface-binding regions, it is plausible to hypothesize that omega-3 fatty acids may have the potential to access the catalytic site under more physiologically relevant, dynamic conditions.

The interpretation of these findings should be considered in light of the methodological limitations inherent to rigid-body docking. This approach treats the protein as a fixed structure, which limits the exploration of induced-fit phenomena and may lead to underestimation of ligand accessibility to conformationally adaptive binding sites. Additionally, solvent effects and entropic contributions were not explicitly modeled, which may further influence the accuracy of the predicted affinities. The elevated RMSD values observed during clustering reflect the exploratory nature of blind docking across the enzyme's entire surface and were not used as a strict convergence criterion in pose selection.

Despite these limitations, blind rigid-body docking was employed in this study as a suitable first-line computational strategy to identify potential binding regions and estimate the relative affinity of ligands toward the target protein. This method is widely used for preliminary screening due to its efficiency, simplicity, and ability to generate hypotheses for further validation.

To overcome the limitations described above, flexible docking protocols were subsequently applied in the present study to allow structural adaptation of the active site. This approach enables evaluation of whether AA, DHA and EPA can access the catalytic pocket under conditions that better account for induced-fit effects.

Docking protocol validation

Re-docking of the co-crystallized molecule FLC (citrate ion) into COX-1 resulted in a close reproduction of the experimental binding pose, with RMSD of 1.739 Å between the crystallographic pose of FLC and the top-ranked re-docked conformation.

These results support the geometric reliability of the docking setup and justify its application for subsequent comparative docking analyses.

Flexible docking results

To further refine the docking analysis, flexible docking was performed to account for the conformational adaptability of amino acid residues within the COX-1 active site. In contrast to the blind docking approach, flexible docking enables selected residues in the binding pocket to move during the simulation, providing a more realistic representation of enzyme-ligand interactions.

The results of flexible docking, presented in Table 2, show binding energies consistent with those

obtained from blind docking, but with generally more favorable (lower) energy values, reflecting improved accommodation of the ligands within the active site. Among the tested compounds, AA exhibits a binding energy of –9.24 kcal/mol, confirming its strong affinity toward the COX-1 catalytic pocket. In comparison, EPA and DHA display binding energies of –8.67 kcal/mol and –8.53 kcal/mol, respectively.

These results suggest that both ω-3 fatty acids can adopt binding poses within the catalytic pocket that overlap with key substrate-interacting regions, indicating a potential for competitive interactions at the molecular level. The observed RMSD values reflect the conformational spread of docked poses within the catalytic site. AA and EPA show relatively lower values (RMSD = 3.715 Å and 3.901 Å, respectively), indicating more convergent clustering, whereas DHA shows a larger deviation (RMSD = 5.368 Å), consistent with its greater conformational freedom. Despite this difference in conformational spread, all three ligands achieve substantially improved binding energies under the flexible protocol (nanomolar-range Ki), with AA and EPA showing the most favorable ΔG.

Table 2. Summary of flexible docking results for DHA, EPA, and AA with COX-1.

Parameter	**DHA**	**EPA**	**AA**
RMSD of docked conformations (clustering), Å	5.368	3.901	3.715
Estimated free energy of binding (ΔG), kcal/mol	-8.73	-9.03	-9.09
Estimated inhibition constant (Ki, 298.15 K), nM (nanomolar)	398.60	239.03	216.87
Final intermolecular energy, kcal/mol	-13.20	-13.21	-13.57
• *Ligand–fixed receptor, kcal/mol*	-11.36	-8.63	-8.66
– *vdW + H-bond + desolvation, kcal/mol*	-11.32	-8.62	-8.66
– *Electrostatic, kcal/mol*	-0.04	-0.01	+0.01
• *Ligand–flexible residues, kcal/mol*	-1.84	-4.58	-4.91
– *vdW + H-bond + desolvation, kcal/mol*	-1.85	-4.42	-4.87
– *Electrostatic, kcal/mol*	+0.00	-0.16	-0.04
Final total internal energy, kcal/mol	-15.19	-12.92	-12.72
• *Ligand internal energy, kcal/mol*	-1.40	-0.86	-0.67
• *Ligand–fixed receptor, kcal/mol*	-13.54	-11.68	-11.96
• *Ligand–flexible residues, kcal/mol*	-0.25	-0.38	-0.09
Torsional free energy, kcal/mol	+4.47	+4.18	+4.47
Unbound system energy, kcal/mol	-15.19	-12.92	-12.72

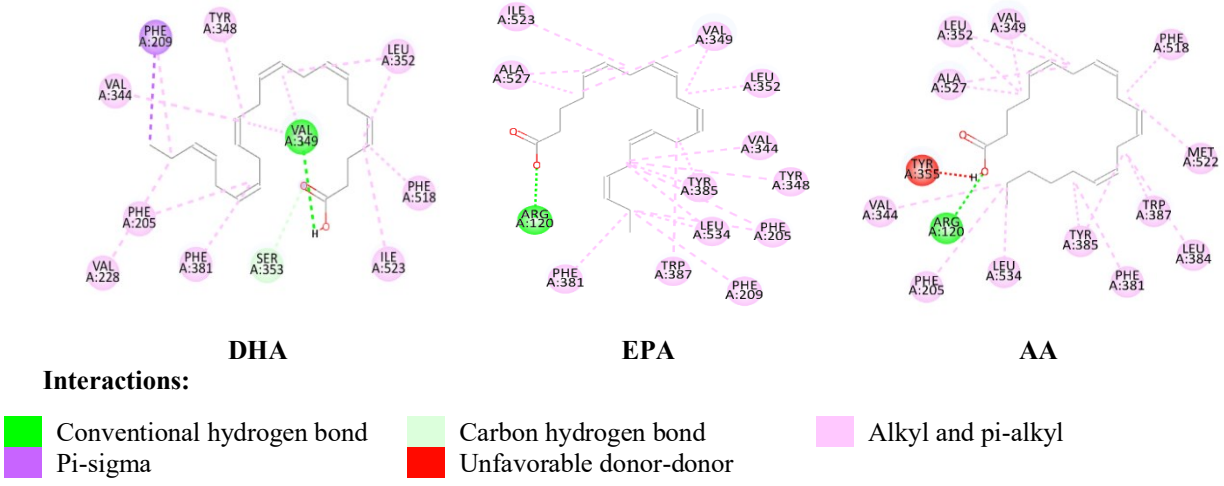

Figure 2. Two-dimensional interaction diagrams from flexible docking of docosahexaenoic acid (DHA), eicosapentaenoic acid (EPA), and arachidonic acid (AA) bound to COX-1, illustrating conventional hydrogen bonds (green) and alkyl interactions (pink).

The larger RMSD for DHA likely reflects its greater conformational freedom (longer, more unsaturated chain) and may correspond to an alternative but still energetically favorable binding mode. Collectively, the flexible docking results support the notion that ω-3 fatty acids can access and be accommodated by the COX-1 catalytic region under receptor flexibility, although the exact orientation and contacts differ among ligands.

In the flexible docking simulations, all three ligands localized within the hydrophobic channel leading to the cyclooxygenase catalytic site of COX-1, establishing key contacts with residues known to participate in substrate anchoring and catalysis. The ligand-protein interaction profiles for DHA, EPA, and AA are shown in Figure 2. The inclusion of receptor flexibility allows the side chains of several residues to adjust their conformations, resulting in tighter fitting and improved complementarity between the ligands and the binding pocket compared to rigid-body docking.

In the flexible docking simulations, AA, EPA, and DHA all localized within the COX-1 catalytic channel, maintaining interactions with residues critical for substrate anchoring and catalysis. AA, used as the reference substrate, forms the characteristic hydrogen bonds between its carboxylate terminus and ARG120 and TYR355, while engaging the hydrophobic residues PHE205, VAL344, LEU534, TYR385, PHE381, LEU384, TRP387, MET522, PHE518, VAL349, LEU352 and ALA527. EPA adopts a nearly identical pose, preserving the hydrogen bond with ARG120 and forming additional alkyl interactions with PHE209, TYR348 and ILE523. In contrast, DHA exhibits a more extended conformation due to its higher degree of unsaturation. It retained a stable hydrogen bond but with VAL349, formed compensatory polar contacts with SER353, and established hydrophobic interactions with PHE381, PHE205, VAL228, VAL344, PHE209, TYR348, LEU352, PHE518 and ILE523. Despite its greater torsional flexibility and higher RMSD, DHA remains anchored through conserved interactions with VAL349 and SER353, confirming its compatibility with the catalytic environment and supporting the view that ω-3 fatty acids can competitively engage the COX-1 active site in a manner comparable to arachidonic acid.

These results indicate that both EPA and DHA can occupy the COX-1 catalytic site, with EPA closely mimicking the reference substrate AA and DHA adopting an alternative yet stable orientation. The observed hydrogen bonding and hydrophobic contacts with key residues support a potential competitive mechanism, although the distinct conformations of DHA highlight the influence of chain flexibility on binding dynamics. Considering the limitations of docking simulations, including neglect of solvent effects and entropic contributions, further studies using molecular dynamics and experimental validation are necessary to confirm these interactions and clarify their functional relevance in COX-1 modulation.

Comparative analysis

Comparison between blind and flexible docking outcomes reveals a clear progression from surface-level association to catalytically relevant binding. In the blind docking simulations, all three fatty acids occupied similar peripheral regions on the COX-1 surface rather than the canonical catalytic pocket. This spatial overlap suggests that the molecules share comparable physicochemical properties governing initial enzyme recognition and surface adhesion. However, the absence of interactions with the key residues ARG120, TYR385, and SER530 indicated that these poses likely represent preliminary, non-productive associations.

When receptor flexibility was introduced, the binding profiles changed substantially. The flexible docking protocol allowed rearrangement of side chains surrounding the active site, enabling all three ligands to access the catalytic channel. Importantly, the binding energies inverted their relative order: while AA exhibited the weakest binding in the rigid-body scenario, it became the most strongly bound ligand under flexible conditions ($\Delta G = -9.09$ kcal/mol), followed closely by EPA (−9.03 kcal/mol) and DHA (−8.73 kcal/mol). This reversal highlights the influence of local conformational adaptation on ligand accommodation and suggests that rigid docking may underestimate true binding affinity for flexible active sites such as COX-1.

The RMSD values (3.7–5.4 Å) reflect the conformational spread of docked poses within the catalytic groove, with AA and EPA showing more convergent clustering and DHA exhibiting greater conformational variability consistent with its longer, more unsaturated chain. The consistent anchoring of the carboxylate group to ARG120 and, in some cases, TYR355 and SER530, confirms productive alignment along the catalytic axis. The energetic improvement of approximately 1-2 kcal/mol for EPA and DHA relative to their rigid-body poses reflects enhanced hydrophobic packing and steric complementarity within the enzyme cavity.

The observed similarities in binding positions and interaction energies among arachidonic, eicosapentaenoic, and docosahexaenoic acids can be rationalized by their close structural and electronic

resemblance, which inherently dictates a comparable pattern of molecular recognition within the COX-1 binding region. Their shared amphiphilic character – defined by a polar carboxylate head and a flexible hydrophobic tail – promotes analogous anchoring near ARG120 and alignment toward the catalytic TYR385–SER530 dyad. These consistent binding profiles across blind and flexible docking simulations reinforce the notion that all three fatty acids may engage the enzyme through similar physicochemical mechanisms, despite differences in flexibility and unsaturation degree. Nevertheless, the computational results presented here serve primarily as predictive evidence and require further validation through biochemical and kinetic assays to confirm the physiological relevance of these interactions.

CONCLUSION

The combined results of blind and flexible docking analyses provide complementary insights into the molecular recognition of COX-1 by arachidonic acid and the omega-3 fatty acids eicosapentaenoic acid and docosahexaenoic acid. While blind docking simulations identify peripheral surface-binding regions shared among all three ligands, flexible docking reveals their capacity to occupy the catalytic channel when receptor mobility is permitted. The restoration of key interactions with ARG120, TYR355, and SER530 under flexible conditions demonstrates that both EPA and DHA can adopt conformations comparable to the native substrate and potentially compete for access to the active site.

Energetically, the small differences in binding free energy ($\Delta G \approx 1–2$ kcal/mol) between the ligands suggest similar affinities toward the catalytic pocket, reflecting their shared amphiphilic architecture and structural homology. The comparable binding orientations and overlapping interaction networks observed for the three fatty acids support the hypothesis that omega-3 compounds may modulate COX-1 activity through competitive mechanisms.

These findings contribute to the growing body of evidence that omega-3 fatty acids possess intrinsic potential to interfere with arachidonic acid metabolism, thereby influencing prostaglandin biosynthesis and inflammatory signaling. However, as docking simulations represent theoretical approximations of molecular interactions, further *in vitro* and *in vivo* studies such as enzyme inhibition assays, kinetic evaluations, and structural analyses are required to validate the predicted binding modes and clarify the physiological implications of these interactions.

REFERENCES

1. K. K. Reddy, V. K. Vidya Rajan, A. Gupta, P. Aparoy, P. Reddanna, *BMC Res. Notes*, **8**, 152 (2015). https://doi.org/10.1186/s13104-015-1101-4
2. R. K. Vishwakarma, D. S. Negi, *International Journal of Pharmaceutical Sciences and Research*, **11** (8), 3544 (2020).
3. S. Wan, P. V. Coveney, *Journal of Computational Chemistry*, **30** (7), 1038 (2009). https://doi.org/10.1002/jcc.21130
4. C. A. Rouzer, L. J. Marnett, *Chem Rev.*, **120** (15), 7592 (2020). http://doi.org/10.1021/acs.chemrev.0c00215
5. A. J. Vecchio, D. M. Simmons, M. G. Malkowski, *Journal of Biological Chemistry*, **285** (29), 22152 (2010). http://doi.org/10.1074/jbc.m110.119867
6. L.L.C. Schrödinger, Docking and Scoring. https://www.schrodinger.com/life-science/learn/white-papers/docking-and-scoring/
7. S. C. Dyall, *Front. Aging Neurosci.*, **7** (52), (2015). http://doi.org/10.3389/fnagi.2015.00052
8. U. N. Das, *Current Pharmaceutical Biotechnology*, **7** (6), 467 (2006). https://doi.org/10.2174/138920106779116856
9. M. J. Calvo, M. S. Martínez, W. Torres, M. Chávez-Castillo, E. Luzardo, N. Villasmil, J. Salazar, M. Velasco, V. Bermúdez, *Vessel Plus*, **1**, 116 (2017). http://dx.doi.org/10.20517/2574-1209.2017.14
10. Y. Zhang, Y. Liu, J. Sun, W. Zhang, Z. Guo, Q. Ma, *MedComm*, **4** (5), e363 (2023). https://doi.org/10.1002/mco2.363
11. L. Dong, H. Zou, C. Yuan, Y. H. Hong, D. V. Kuklev, W. L. Smith, *J. Biol. Chem.*, **291** (8), 4069 (2016). http://doi.org/10.1074/jbc.M115.698001
12. A. S. Roman, J. Schreher, A. P. Mackenzie, P. W. Nathanielsz, *Am. J. Obstet. Gynecol.*, **195** (6), 1693 (2006). http://doi.org/10.1016/j.ajog.2006.04.009
13. W. L. Smith, M. G. Malkowski, *J. Biol. Chem.*, **294** (5), 1697 (2019).
14. P. C. Agu, C. A. Afiukwa, O. U. Orji, E. M. Ezeh, I. H. Ofoke, C. O. Ogbu, E. I. Ugwuja, P. M. Aja, *Scientific Reports,* **13**, 13398 (2023). https://doi.org/10.1038/s41598-023-40160-2
15. P. H. M. Torres, A. C. R. Sodero, P. Jofily, F. P. Silva-Jr, *Int. J. Mol. Sci.,* **20** (18), 4574 (2019). http://doi.org/10.3390/ijms20184574
16. I. A. Guedes, C. S. de Magalhães, L. E. Dardenne, *Biophysical Reviews*, **6**, 75 (2014). https://doi.org/10.1007/s12551-013-0130-2
17. E. Mateev, B. Angelov, M. Kondeva-Burdina, I. Valkova, M. Georgieva, A. Zlatkov, *Farmacia*, **70** (6), 1126 (2022). http://doi.org/10.31925/farmacia.2022.2.21
18. C. Hetényi, D. van der Spoel, *Protein Science*, **20** (5), 880 (2011) https://doi.org/10.1002/pro.618
19. C. Hetényi, D. van der Spoel, *FEBS Letters*, **580** (5), 1447 (2006)
20. E. Mateev, M. Kondeva-Burdina, M. Georgieva, A. Mateeva, I. Valkova, V. Tzankova, A. Zlatkov, *Sci.*

Pharm., **92** (2), 18 (2024). https://doi.org/10.3390/scipharm92020018
21. G. M. Morris, R. Huey, W. Lindstrom, M. F. Sanner, R. K. Belew, D. S. Goodsell, A. J. Olson, *Journal of Computational Chemistry*, **30** (16), 2785 (2009). https://doi.org/10.1002/jcc.21256
22. L. G. Ferreira, R. N. Dos Santos, O. Glaucius, A. D. Andricopulo, *Molecules,* **20** (7), 13384 (2015). https://doi.org/10.3390/molecules200713384
23. S. Kim, J. Chen, T. Cheng, A. Gindulyte, J. He, S. He, Q. Li, B. A. Shoemaker, P. A. Thiessen, B. Yu, L. Zaslavsky, J. Zhang, E. E. Bolton, *Nucleic Acids Research*, **49** (D1), D1388 (2021). https://doi.org/10.1093/nar/gkaa971
24. M. D. Hanwell, D. E. Curtis, D. C. Lonie, T. Vandermeersch, E. Zurek, G. R. Hutchison, *Journal of Cheminformatics*, **4**, 17 (2012). https://doi.org/10.1186/1758-2946-4-17
25. S. K. Burley, C. Bhikadiya, C. Bi, S. Bittrich, L. Chen, G. V. Crichlow, C. H. Christie, K. Dalenberg, L. Di Costanzo, J. M. Duarte, S. Dutta, Z. Feng, S. Ganesan, D. S. Goodsell, S. Ghosh, R. K. Green, V. Guranović, D. Guzenko, B. P. Hudson, C. L. Lawson, Y. Liang, R. Lowe, H. Namkoong, E. Peisach, I. Persikova, C. Randle, A. Rose, Y. Rose, A. Sali, J. Segura, M. Sekharan, C. Shao, Y.-P. Tao, M. Voigt, J. D. Westbrook, J. Y. Young, C. Zardecki, M. Zhuravleva, *Nucleic Acids Research*, **49** (D1), D437 (2021). https://doi.org/10.1093/nar/gkaa1038
26. M. Miciaccia, B. D. Belviso, M. Iaselli, G. Cingolani, S. Ferorelli, M. Cappellari, P. Loguercio Polosa, M. G. Perrone, R. Caliandro, A. Scilimati, *Scientific Reports,* **11**, 4312, (2021). https://doi.org/10.1038/s41598-021-83438-z
27. E. F. Pettersen, T. D. Goddard, C. C. Huang, E. C. Meng, G. S. Couch, T. I. Croll, J. H. Morris, T. E. Ferrin, *Protein Science,* **30** (1), 70 (2021). https://doi.org/10.1002/pro.3943
28. Dassault Systèmes BIOVIA, Discovery Studio Visualizer, Version 21.1.0. San Diego: Dassault Systèmes BIOVIA Corp., 2020. Available at: https://discover.3ds.com/discovery-studio-visualizer-download
29. A. C. Rufer, *Drug Discovery Today*, **26** (4), 875 (2021). https://doi.org/10.1016/j.drudis.2021.01.006
30. S. F. Sousa, P. A. Fernandes, M. J. Ramos, *Proteins: Structure, Function, and Bioinformatics*, **65** (1), 15 (2006). https://doi.org/10.1002/prot.21082
31. H. Zou, C. Yuan, L. Dong, R. S. Sidhu, Y. H. Hong, D. V. Kuklev, W. L. Smith, *Journal of Lipid Research*, **53** (7), 1336 (2012). https://doi.org/10.1194/jlr.M026856